Supporting Information

Highly stable supercapacitive performance of the one-dimensional (1D) brookite TiO_2 nanoneedles

Rupesh S. Devan[a,b,c]*, Yuan-Ron Ma[c]*, Ranjit A. Patil[c], and Schmidt-Mande Lukas[d]

[a]Department of Physics, Savitribai Phule Pune (Formerly, University of Pune), Pune 411007, India
[b]Centre for Physical Sciences, School of Basic and Applied Sciences, Central University of Punjab, Bathinda, 151001, India
[c]Department of Physics, National Dong Hwa University, Hualien 97401, Taiwan, R.O.C.
[d]Department of Physics, University of Konstanz, 78457 Constance, Germany.

*C***orresponding authors**:

Dr. Rupesh S. Devan, Associate Professor, Centre for Physical Sciences, School of Basic and Applied Sciences, Central University of Punjab, Bathinda, Punjab 151001, India. E-mail: devan_rs@yahoo.co.in
Prof. Yuan-Ron Ma, Department of Physics, National Dong Hwa University, Hualien 97401, Taiwan. E-mail:ronma@mail.ndhu.edu.tw

Galvanostatic charging-discharging:

The galvanostatic charging-discharging (Fig. S1,) of 1D β-TiO_2 nanoneedles was studied at various current densities of 166.7, 250, 333.3 and 416.7 µA/g. Obviously, the charging curves were relatively symmetric to their discharge counterpart implying that a highly reversible ion transportation is efficiently taking place along the textural boundaries of 1D β-TiO_2 nanoneedles.

The specific capacitance from the galvanostatic charging-discharging was calculated using equation –

$$C_s = \frac{I}{m \cdot (dV/dt)} \qquad \text{--- (S1)}$$

where, C_s is specific capacitance (F/g), I is the applied current (A), m is the mass of the active material (g), and dV/dt is the slope of the discharge curve (V/s). The C_s derived from the charge-discharge test (Fig. S1(b)) maintaining good linearity and gradually decreasing with increas in the current density from 166.7 to 416.7 μA/g, since the ion accessibility is limited to the surface of the 1D β-TiO_2 nanoneedles on the relevant timescale. The C_s value of 192.2 mF/g gained at a current density of 166.7 μA/g was decreased up to 27.6 mF/g at 417.7 μA/g. To our knowledge, these C_s values of 1D β-TiO_2 nanoneedles are larger than those achieved by brookite TiO_2 thin films and nanostructures. These values are comparable those obtained from anatase, [1] rutile [2] and hexagonal [3] TiO_2 structures. Moreover, 1D β-TiO_2 nanoneedles showed a more rapid ion diffusion mechanism in comparison to TiO_2 nanoparticles and its multilayer film with graphene, [4] TiO_2@C core-shell nanowires, [5] and anatase to rutile transformed TiO_2 nanotubes. [6]

The energy density (E), power density (P), and coulombic efficiency (η) of the supercapacitor devices was calculated from the equations,

$$E = \frac{1}{2} \times C_s \times (\Delta V)^2 \frac{1000}{3600} \qquad \text{--- (S2)}$$

$$P = \frac{1}{2} \times \frac{C_s \times (\Delta V)^2 \times 1000}{\Delta t_d} = \frac{E}{\Delta t} 3600 \qquad \text{--- (S3)}$$

$$\eta(\%) = \frac{\Delta t_d}{\Delta t_c} \times 100 \qquad \text{--- (S4)}$$

where, E is the energy density (Wh/Kg), C_s is specific capacitance obtained from Eq. (3), ΔV is the discharge voltage range (V) on the potential window, P is the power density (W/Kg), η is the columbic efficiency, and Δt_d and Δt_c are discharge and charging time, respectively. The calculated energy density and power density of the 1D β-TiO_2 nanoneedles are 3.04 Wh/Kg, and 206.09 W/Kg, respectively, at a scan rate of 15 mV/s. To demonstrate the overall performance of 1D B-TiO_2 nanoneedles, a Ragone plot is shown in Fig. S2. A Ragone plot manifests a energy density and power density of 3.04Wh/Kg and 1683W/Kg, respectively, which is better than the previous reported for anatase TiO_2 nanotubes, [1] vertically aligned rutile TiO_2 nanorods, [2] microwave assisted graphene-TiO_2 hybrid nanostructures, [7] and hybrid supercapacitor fabricated with the carbon nanotube (CNT) cathode and TiO_2 nanowire anode. [8] The columbic efficiency of 98 % is obtained from 1D β-TiO_2 nanoneedles and is mainly attributed to the increased contributions of large surface area and textural boundaries. These results clearly demonstrate a new dimension of the 1D β-TiO_2 nanoneedles for the development of high stable supercapacitor of long cycle lifetime.

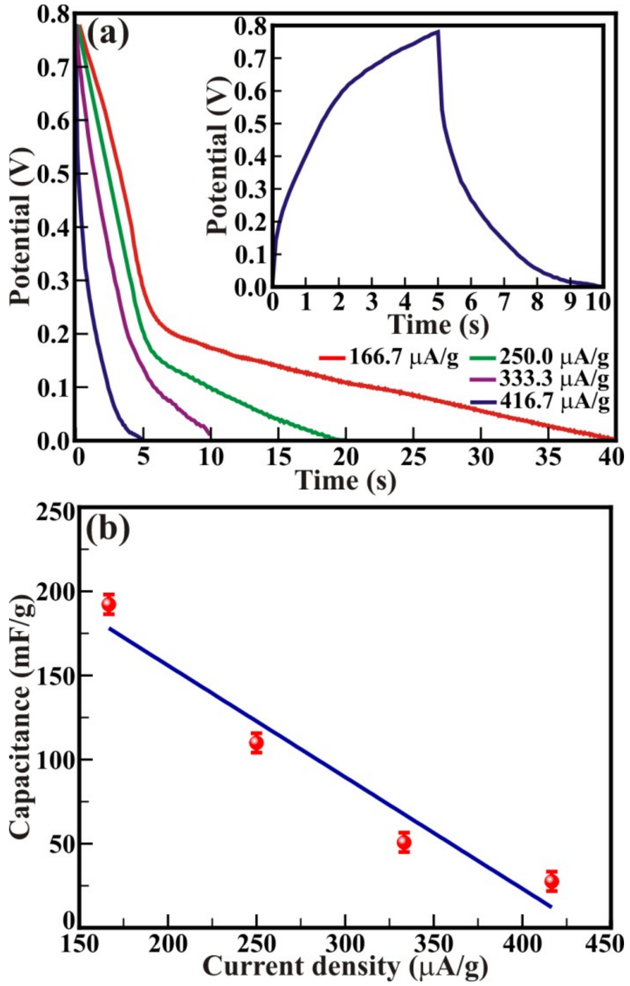

Fig. S1 Galvanostatic discharge curves of the 1D β-TiO_2 nanoneedles collected at various current densities within the limiting potential of 0 to 0.8 V. (b) The specific capacitance for various current densities calculated from discharging curves.

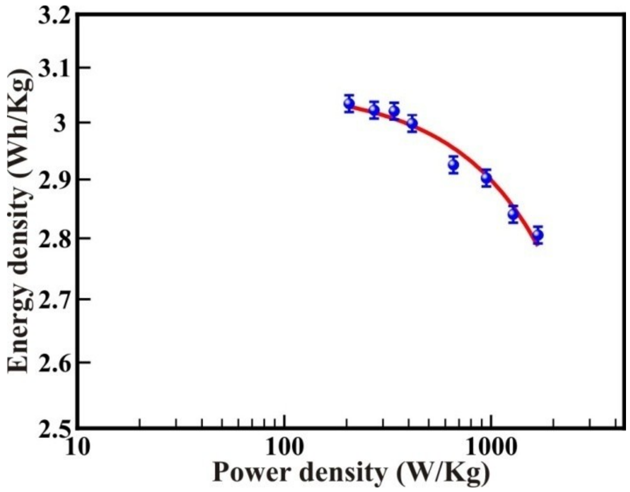

Fig. S2 Ragone plot derived from CV to determine the performance of the 1D β-TiO_2 nanoneedles.

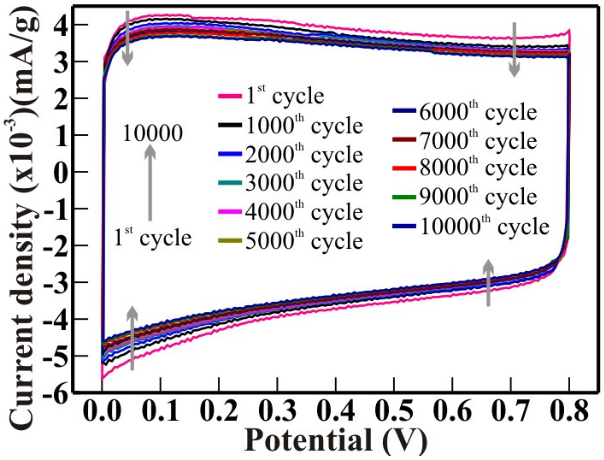

Fig. S3 Figure shows selected cyclic voltammograms obtained at scan rate of 100 mV/s for number cycles from 1 to 10,000 cycles.

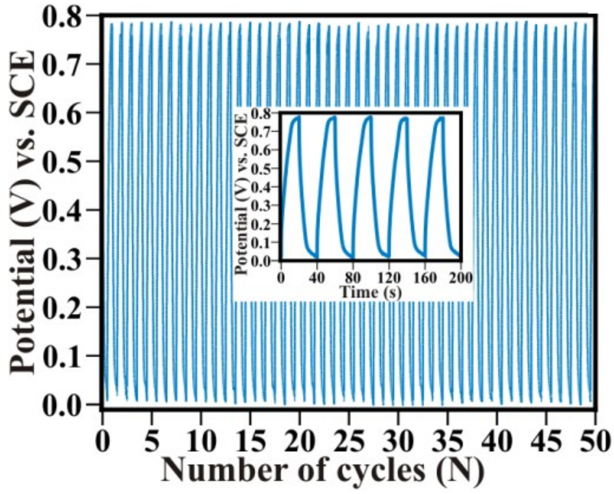

Fig. S4 First 50 glavanostatic charging-discharging cycles extracted out of 5,000 cycles obtained at current density of 250 µA/g. Inset shows first five cycles.

Table 1 – The 1D β-TiO_2 nanoneedles shows better stability than the pure and hybrid metal-oxide nanostructures listed in the table below.

Sr. No.	Electrode Materials	Capacitance reduction (%)	Number of cycles	Ref. No.
1.	V_2O_5 nanowires	~ 50.0 %	5000	[9]
2.	NiO porous microtubes	~ 22.6 %	2000	[10]
3.	NiO nanoparticle tube	~ 48.0 %	1000	[11]
4.	Co_3O_4 nanowires	~ 15.0 %	1000	[12]
5.	Co_3O_4 hollow nanotube	~ 9.0 %	1000	[13]
6.	α-MnO_3 nanobelts	~ 5.0 %	500	[14]
7.	NiO@MnO_2 microtube	~ 18.3 %	2000	[10]
8.	Graphene@V_2O_5 nanobelts	~12.0 %	5000	[15]
9.	MnO_2 nanowires/ZnO nanorods	~ 6.5 %	1000	[16]
10.	V_2O_5 doped α-Fe_2O_3 nanotubes	~ 24.5 %	200	[17]

11.	Carbon coated V_2O_5 nanorods	~ 24.0 %	1000	[18]
12.	V_2O_5 nanoporous network	~ 24.0 %	600	[19]
13.	SnO_2 Nanosheets	~ 58.2 %	6000	[20]
14.	Co_3O_4 nanosheets	~ 31.0 %	1000	[21]
15.	Co_3O_4 ultrathin nanosheets	~ 21.5 %	2000	[22]
16.	MnO_2 nanosheets	~ 26.5 %	2000	[10]
17.	SnO_2@Co_3O_4 core-shell nanosheets	~ 41.7 %	6000	[20]
18.	MnO_2 nanoparticles	~ 22.8 %	1000	[23]
19.	Ni@NiO core-shell nanoparticulate tube	~ 19.0 %	1000	[11]
20.	SnO_2@MnO_2 nanoparticles	~ 18.9 %	1000	[23]
21.	Ppy/GO/ZnO nanocomposite on Ni-Fome	~ 97.0 %	1000	[24]
22.	$Ni(OH)_2$/Graphene and RuO_2/Graphene	~ 8.0 %	5000	[15]
23.	MnO_2 grafted V_2O_5 nanostructure	~ 11.0 %	500	[26]
24.	NiO-CeO_2 nanoparticles composites	~ 15.0 %	1000	[27]

References:

[1] X. H. Lu, G. M. Wang, T. Zhai, M. H. Yu, J. Y. Gan, Y. X. Tong and Y. Li, *Nano Lett.*, 2012, **12**, 1690-1696.

[2] A. Ramadoss and S. J. Kim, *J. Alloy. Compd.*, 2013, **561**, 262-267.

[3] H. Zhou and Y. Zhang, *J. Phys. Chem. C*, 2014, **118**, 5626-5636.

[4] W. W. Liu, X. B. Yan and Q. J. Xue, *J. Mater. Chem. C*, 2013, **1**, 1413-1422.

[5] H. M. Zheng, T. Zhai, M. H. Yu, S. L. Xie, C. L. Liang, W. X. Zhao, S. C. I. Wang, Z. S. Zhang and X. H. Lu, *J. Mater. Chem. C*, 2013, **1**, 225-229.

[6] M. Salari, K. Konstantinov and H. K. Liu, *J. Mater. Chem.*, 2011, **21**, 5128-5133.

[7] A. Ramadoss, and S. J. Kim *Carbon*, 2013, **63**, 434-445.

[8] Q. Wang, Z. H. Wen and J. H. Li, *Adv. Funct. Mater.*, 2006, **16**, 2141-2146.

[9] Z. Chen, V. Augustyn, J. Wen, Y. W. Zhang, M. Q. Shen, B. Dunn, and Y. F. Lu, Adv. Mater., 2011, 23, 791–795.

[10] J. J. Chen, Y. Huang, C. Li, X. F. Chen, X. Zhang, Appl. Surf. Sci., 2016, 360, 534–539.

[11] Q. Li, C. L. Liang, X. F. Lu, Y. X. Tong, and G. R. Li, J. Mater. Chem. A, 2015, 3, 6432–6439

[12] W. W. Liu, X. Li, M. H. Zhu, X. He, J. Power Source., 2015, 282, 179-186.

[13] M. M. Yao, Z. H. Hu, Z. J. Xu, and Y. F. Liu, J. Alloys Comp., 2015, 644, 721-728.

[14] J. B. Jiang, J. L. Liu, S. J. Peng, D. Qian, D. M. Luo, Q. F. Wang, Z. W. Tian, and Y. C. Liu, J. Mater. Chem. A, 2013, 1, 2588-2594.

[15] M. Lee, S. K. Balasingam, H. Y. Jeong, W. G. Hong, H. B. R. Lee, B. H. Kim, & Y. Jun, Sci. Rep., 2015, 5, 8151.

[16] S. Z. Li, J. Wen, X. M. Mo, H. Long, H. N. Wang, J. B. Wang, G. J. Fang, J. Power Sourc., 2014, 256, 206-211.

[17] G. D. Nie, X. F. Lu, J. Y. Lei, Z. Q. Jiang, and C. Wang, J. Mater. Chem. A, 2014, 2, 15495–15501.

[18] B. Saravanakumar, K. K. Purushothaman, and G. Muralidharan, J. Electroanal. Chem., 2015, 758, 111-116.

[19] B. Saravanakumar, K. K. Purushothaman, and G. Muralidharan, ACS Appl. Mater. Interfaces 2012, 4, 4484−4490.

[20] Y. Liu, Y. Jiao, B. S. Yin, S. W. Zhang, F. Y. Qu, and X. Wu, J. Mater. Chem. A, 2015, 3, 3676-3682.

[21] S. J. Deng, X. C. Xiao, G. Chen, L. H. Wang, Y. Wang, Electrochim. Acta, 2016, 196, 316–327.

[22] X. H. Wang, S. W. Yao, X. X. Wu, Z. J. Shi, H. X. Sun, R. H. Que, RSC Adv., 2015, 5, 17938-17944.

[23] Y. Q. Zhang, and Y. Mo, Electrochim. Acta, 2014, 142, 76–83.

[24] W. K. Chee, H. N. Lim, and N. M. Huang, Int. J. Energy Res., 2015, 39, 111-119.

[25] H. L. Wang, Y. Y. Liang, T. Mirfakhrai, Z. Chen, H. S. Casalongue, H. J. Dai, Nano Res., 2011, 4, 729-736.

[26] B. Saravanakumar, K. K. Purushothaman, and G. Muralidharan, Cryst. Eng. Comm., 2014, 16, 10711–10720.

[27] N. Padmanathan, and S. Selladurai, Ionics, 2014, 20, 409–420.